JOURNAL OF VIROLOGY, Sept. 2000, p. 8018–8027 Vol. 74, No. 17
0022-538X/00/$04.00+0

Targeted Infection of Endothelial Cells by Avian Influenza Virus A/FPV/Rostock/34 (H7N1) in Chicken Embryos

ANKE FELDMANN,[1] MARTIN K.-H. SCHÄFER,[2] WOLFGANG GARTEN,[1] AND HANS-DIETER KLENK[1]*

Institut für Virologie[1] and Institut für Anatomie und Zellbiologie,[2] Philipps-Universität, Marburg, Germany

Received 15 February 2000/Accepted 26 May 2000

The tissue tropism and spread of infection of the highly pathogenic avian influenza virus A/FPV/Rostock/34 (H7N1) (FPV) were analyzed in 11-day-old chicken embryos. As shown by in situ hybridization, the virus caused generalized infection that was strictly confined to endothelial cells in all organs. Studies with reassortants of FPV and the apathogenic avian strain A/chick/Germany/N/49 (H10N7) revealed that endotheliotropism was linked to FPV hemagglutinin (HA). To further analyze the factors determining endotheliotropism, the HA-activating protease furin was cloned from chicken tissue. Ubiquitous expression of furin and other proprotein convertases in the chick embryo indicated that proteolytic activation of HA was not responsible for restriction of infection to the endothelium. To determine the expression of virus receptors in embryonic tissues, histochemical analysis of α2,3- and α2,6-linked neuraminic acid was carried out by lectin-binding assays. These receptors were found on endothelial cells and on several epithelial cells, but not on tissues surrounding endothelia. Finally, we analyzed the polarity of virus maturation in endothelial cells. Studies on cultured human endothelial cells employing confocal laser scanning microscopy revealed that HA is specifically targeted to the apical surface of these cells, and electron microscopy of embryonic tissues showed that virus maturation occurs also at the luminar side. Taken together, these observations indicate that endotheliotropism of FPV in the chicken embryo is determined, on one hand, by the high cleavability of HA, which mediates virus entry into the vascular system, and, on the other hand, by restricted receptor expression and polar budding, which prevent spread of infection into tissues surrounding endothelia.

Influenza A viruses are found in humans, pigs, and several other mammals as well as in many birds. It is generally believed that the mammalian viruses emerge from the large reservoir of avian strains comprising 15 hemagglutinin (HA) and 9 neuraminadase (NA) subtypes (42). Most influenza A viruses cause local infection that is confined to the respiratory tract or, in the case of some avian strains, to the gut. The avian viruses showing this type of infection usually have low pathogenicity or are completely apathogenic. In contrast, some avian strains belonging to subtypes H5 and H7 cause generalized infection. These viruses are highly pathogenic, killing the birds within a few days. An important determinant for these differences in spread of infection is cleavage activation of HA, which, in the case of the pathogenic strains, is exerted by ubiquitous proteases, such as the proprotein convertase furin, whereas strains causing localized infection are activated by proteases expressed specifically in the respective tissues (for review, see reference 16).

Until recently, it was believed that the highly pathogenic avian strains are not transmitted to humans. However, in the course of an H5N1 outbreak among chickens, several human infections with a high case fatality rate were observed in 1997 in Hong Kong (6, 35). Furthermore, an H7N7 virus was isolated in 1996 from a human with milder disease symptoms that proved to be closely related to the avian isolate A/turkey/Ireland/PV74/95 (1, 18). These observations demonstrate that H5 and H7 strains can be transmitted from birds to humans without an intermediate host and without reassortment and, even more importantly, that the pathogenetic potential of these viruses as determined by HA is preserved to some extent in the new host.

As a result of the systemic infection caused by the pathogenic H5 and H7 strains in birds, virus can be recovered from many organs. Large hemorrhages distributed all over the body, edema, and cutaneous ischemia are major symptoms of the disease. The final stage of the infection can be characterized by the emergence of neurological signs, such as photophobia and dullness (13, 20). Although hemorrhages and edema indicate an affliction of the vascular system, only few data are available pertaining to cell tropism in the natural host. The virulent influenza strain A/turkey/Ontario/7732/66 (H5N9), for example, has a pronounced effect on lymphocytes and lymphoid tissue of its avian host (39, 40). Another pathogenic strain, A/turkey/England/50-92/91 (H5N1), strongly attacks the cardiovascular system of the birds by predominantly infecting myocytes and endothelial cells of the heart muscle (17). Similar results have been obtained when chickens were experimentally infected with avian and human isolates obtained during the H5N1 outbreak in 1997 in Hong Kong (34). Conclusions on tissue and cell tropism drawn from investigations using one strain are not necessarily applicable to others.

Although the importance of HA cleavability for spread of infection in the organism is beyond doubt, cell tropism is likely to be controlled by multiple virus and host factors. Polarity of virus budding may be such a determinant, as indicated by studies on Sendai virus. Wild-type Sendai virus, which is pneumotropic in mice, has been found to bud strictly from the luminal side of polarized epithelial cells, whereas a pantropic mutant showed bipolar budding, allowing virus spread into adjacent tissues (37, 38). Influenza virus also buds specifically from the apical side of polarized epithelial cells in culture (23), but little is known about the biological significance of the budding polarity of this virus in vivo. Binding of HA to the receptor may be another determinant controlling spread of

* Corresponding author. Mailing address: Institut für Virologie, Postfach 2360, 35011 Marburg, Germany. Phone: 06421/28 66253. Fax: 06421/28 68962. E-mail: klenk@mailer.uni-marburg.de.

infection in the organism. It is well known from the work of several groups that influenza viruses differ in their receptor specificity. For instance, it has been reported that most avian influenza viruses recognize preferentially neuraminic acid bound by α2,3-linkage to galactose (NeuAc-α2,3-Gal), whereas human influenza viruses prefer NeuAc-α2,6-Gal (5, 10, 24, 25). This difference is important for host tropism, but it is not known whether receptor binding plays a role in cell tropism within a given organism.

In the present study, we have analyzed spread of infection by the fowl plague virus (FPV) strain A/FPV/Rostock/34 (H7N1) in the chicken embryo. We have found that the virus is strictly endotheliotropic in this host. We have also investigated the viral and host factors underlying endotheliotropism.

MATERIALS AND METHODS

Viruses. Influenza virus strains A/FPV/Rostock/34 (H7N1) (FPV), A/chick/Germany/N/49 (H10N7) (virus N), reassortants of both influenza virus strains, and strain Indiana of vesicular stomatitis virus (VSV) were used. The generation of the influenza virus reassortants as well as the identification of their genotypes have been described before (26, 31, 32). Seed stocks of influenza virus were grown in the allantoic cavity of 11-day-old embryonated eggs. VSV seed stocks were grown in MDCK cells.

Cloning of chicken furin (gfur) and generation of cRNA probes for PC6a, LPC/PC7, and PACE4 from chicken tissue. The complete *gfur* gene was cloned from a chicken liver cDNA gene bank (Stratagene, La Jolla, Calif., catalog no. 965402) and sequenced (GenBank Z68093). A 331-nucleotide (nt) fragment (nt 533 to 864) of bovine furin (41) (GenBank X75956) labeled with [^{32}P]CTP served as a screening probe. Recombinant vaccinia virus encoding *gfur* (VV:gfur) was generated using the pSC11smaI vector (41). For the other chicken proprotein convertases, riboprobes were generated by reverse transcription (RT)-PCR from chicken liver RNA using oligonucleotide primers derived from the corresponding human genes (hPC5/PC6, GenBank U56387; hLPC/PC7, GenBank U40623; and hPACE4, GenBank M80482). The following primers were used: PC6a, 5′GATGA(C/T)GG(C/A)T(C/T)GAGAGAACCCA(C/T)CCAGATC3′ (529 to 559) and 5′CTCCG(C/A)CCCATTCT(C/A)AC(G/A)CC(G/A)TTCTCAAAG3′ (920 to 890); LPC/PC7, 5′ACTATCAGATCAATGACATCTA3′ (851 to 873) and 5′GTCTCCGCGACGTC3′ (1300 to 1281); and PACE4, 5′CATAAAGTT AGCCATTTCTAT3′ (1574 to 1597) and 5′TTCAGCCTTTTTCTCCCCAGC A3′ (1966 to 1945). The gPC6a fragment (391 nt) (GenBank AJ252169) showed 96% homology to nt 29 to 920 of hPC6a. The gLPC/PC7 fragment (449 nt) (GenBank AJ252170) showed 85% homology to nt 851 to 1300 of hLPC/PC7. The gPACE4 fragment (392 nt) (GenBank AJ25271) exhibited 70% homology to nt 1574 to 1966 of hPACE4. The VEGF receptor 2 probe (Qflk-344-1/351 nt) cloned from quail RNA was kindly provided by Ingo Flamme (Zentrum für Molekulare Medizin, Cologne, Germany). A fragment of 46 nt corresponding to nt 1252 to 1713 of the HA cDNA of A/FPV/Rostock/34 (H7N1) (11) (GenBank M24457) was subcloned into the transcription vector pBluescript KS+. A fragment corresponding to nt 846 to 1300 of the HA gene of A/chick/Germany/N/49 (H10N7) (8) (GenBank M21646) was cloned by RT-PCR using viral RNA into the transcription vector pBluescript KS+.

Tissue preparation. Virus (200 μl, about 10^3 to 10^4 PFU) was injected directly into the allantoic cavity of 11-day-old embryonated eggs. At 18 h after infection, the head, legs, and wings were removed from the embryo and immediately frozen in isopentane at −30 to −50°C on dry ice. Sections (20 μm) were prepared on a cryostat (2800 Frigocut N; Leica, Bensheim, Germany) in sagittal planes. Tissues were stored at −80°C.

In situ hybridization. In situ hybridization was performed according to a reported protocol (29). Briefly, frozen sections were fixed in 4% phosphate-buffered paraformaldehyde solution for 60 min at room temperature and then washed three times in 0.05 M phosphate-buffered saline (PBS; pH 7.4) for 10 min each. Deproteination was carried out with proteinase K (1 μg/ml) for 6 min at 37°C. Slides were transferred to 0.1 M triethanolamine (pH 8.0) and incubated in the same solution containing acetic anhydride (0.25%, vol/vol) for 10 min at room temperature. Sections were washed in PBS and dehydrated in ethanol (50 and 70%). Radioactive cRNA probes were diluted in hybridization buffer (50% formamide, 10% dextran solution, 1× Denhardt's solution, 0.2% [wt/vol] bovine serum albumin, 0.02% [wt/vol] Ficoll 400, 0.02% [wt/vol] polyvinylpyrrolidone, 0.1 mg of yeast RNA per ml, and sheared salmon sperm DNA [0.1 mg/ml]) to a final concentration of 5×10^4 cpm/μl. Dithiothreitol was added to a final concentration of 10 mM. Hybridization mix (30 to 50 μl per slide) was applied, and sections were coverslipped and sealed with rubber cement. The tissue was incubated at 58°C for 16 h in a humid chamber. The coverslips were removed in 2× SSC (1× SSC is 0.15 M NaCl plus 0.015 M sodium citrate). Sections were treated with RNase A (20 μg/ml) and RNase T_1 (1 U/ml) at 37°C for 60 min to remove single-stranded RNA molecules. Successive washes followed at room temperature in 2×, 1×, 0.5×, and 0.2× SSC for 10 min each and in 0.2× SSC at 60°C for 60 min. The tissue was dehydrated and exposed to a Kodak Biomax X-ray film for 1 to 4 days. For microscopic analysis, sections were dipped in Kodak NTB2 nuclear emulsion and stored at 4°C. Following exposure times of from 4 (H7 and H10) to 30 days (VEGF receptor 2 and proteases), autoradiograms were developed in Kodak D19 for 5 min and fixed in Rapid fix (Kodak, Rochester, N.Y.) for 10 min. Tissues were counterstained by hematoxylin-eosin staining.

Lectin binding assays. For detection of NeuAc-α2,3-Gal and NeuAc-α2,6-Gal on the surface of the cells of chicken embryos, a digoxigenin (DIG) glycan differentiation kit (Boehringer, Mannheim, Germany) was used. Sections (200 μm) of uninfected chicken embryos were fixed for 2 min in ice-cold methanol containing 1 mM levamisole (Sigma, Deisenhofen, Germany), a specific inhibitor of endogenous alkaline phosphatase. Sections were then incubated for 12 h with a blocking solution supplied with the kit. The slides were washed twice with TBS buffer (0.05 M Tris-HCl [pH 8.5], 0.15 M NaCl) for 10 min each and once with buffer 1 (TBS, 1 mM $MgCl_2$, 1 mM $CaCl_2$, 1 mM $MnCl_2$). DIG-labeled lectins (*Sambucus nigra* agglutinin [SNA], specific for NeuAc-α2,6-Gal, and *Maackia amurensis* agglutinin [MAA], specific for NeuAc-α2,3-Gal) dissolved in buffer 1 were then incubated with the slides for 2 h. After three washes with TBS, the sections were incubated for 1 h with anti-DIG antibody conjugated to alkaline phosphatase (1:1,000 in TBS). After three washes with TBS, the sections were incubated with buffer 2 (0.1 M Tris-HCl [pH 9.5], 0.05 M $MgCl_2$, 0.1 M NaCl), and the substrate solution NBT/X-phosphate (supplied with the kit) dissolved in buffer 2 containing 1 mM levamisole was applied to the sections. After 5 to 10 min, the reaction was stopped by washing the slides in H_2O. The sections were coverslipped without counterstaining.

Analysis of infected HUVECs on Transwell filters. Polycarbonate filters (1-μm pore size, 2.5 cm in diameter) were coated with 0.1% gelatin for 2 h. Subsequently, the gelatin was cross-linked for 30 min with 2% glutaraldehyde (in PBS) and washed with 70% ethanol. After excessive washing with PBS overnight, filters were put into six-well plates. Primary cultures of endothelial cells from human umbilical cord vein (HUVEC) were prepared by standard methods (12) and seeded on the coated filter in 1.5 ml of medium 199 with 10% fetal calf serum (FCS) (upper compartment) and cultured until confluency (24 to 48 h). The lower compartment contained 2 ml of medium.

For infection, cells were washed with medium 199 with 10% FCS and incubated apically for 1 h at 37°C with egg-grown FPV or MDCK cell-grown VSV at a multiplicity of infection (MOI) of 0.5. After a further washing step, viral inoculum was replaced by medium 199 with 10% FCS. At 4 h postinfection, cells were cooled on ice and washed three times with PBS. Cells were then incubated for 20 min from either the apical or the basolateral side with 1 ml of PBS containing 1.5 mg of Sulfo-NHS-Biotin (Pierce, Rockford, Ill.). At the nonlabeled sides, the filters were always incubated with PBS–0.1 M glycine to inactivate biotin penetrating the pores of the filter. After biotinylation, one washing step with PBS–0.1 M glycine and three additional washes with PBS were performed. The membranes were cut out and incubated on ice for 1 h with radioimmunoprecipitation assay-lysation buffer. The supernatant was cleared by ultracentrifugation (20 min, 40,000 rpm, 4°C, Beckman rotor TLA100.3). Half of the supernatant was incubated with a monoclonal antibody against FPV HA (HA1-2A11H7, generated in the institute) or a polyclonal rabbit antiserum against VSV. Immunoprecipitation and sodium dodecyl sulfate-polyacrylamide gel electrophoresis (SDS-PAGE) under nonreducing conditions followed. The viral proteins were transferred to nitrocellulose (0.4 mA/cm^2 for 1 h). After a blocking step (5% nonfat drymilk in PBS) for 45 min at 4°C, the membrane was washed three times with PBS–0.1% Tween. This was followed by incubation for 45 min with streptavidin-peroxidase (1:2,000 in PBS) and three additional washing steps. Labeled proteins were visualized with the enhanced chemiluminescence detection system Super signal ultra (Pierce).

Immunofluorescence studies. Confluent monolayers of HUVEC grown on filters (see below) were infected with FPV or VSV at an MOI of 0.5. At 4 h postinfection (p.i.), cells were fixed with 2% formaldehyde in PBS for 15 min, washed twice with PBS, and incubated for 1 h with a monoclonal antibody directed against FPV HA (HA1-2A11H7). Subsequently, cells were washed twice with PBS and incubated with specific fluorescein isothiocyanate (FITC)-conjugated antiserum against mouse or rabbit immunoglobulins (Dako, Glostrup, Denmark).

Electron microscopy. The organs of infected chicken embryos were prepared at 18 h p.i. and fixed immediately in ITO buffer according to a reported protocol (15). Subsequently an additional fixation step with OsO_4 was carried out. The tissue was embedded in Epon and ultrathin sections were prepared and contrasted by uranyl acetate and lead citrate prior to microscopic analysis using a Zeiss 109 electron microscope.

RESULTS

Endothelial cells, a target of FPV infection. When 11-day-old chicken embryos were infected via the allantoic route with 10^3 PFU of FPV, they died 18 h p.i. and displayed ubiquitous and extensive subcutaneous hemorrhages. In contrast, embryos infected with virus N, which was used as an "apathogenic"

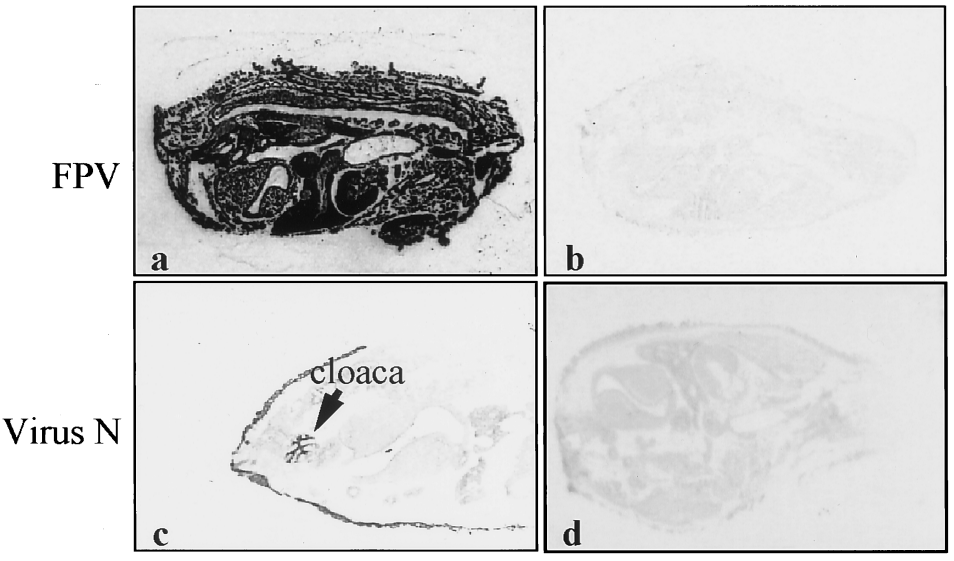

FIG. 1. Spread of FPV and virus N in the chick embryo. Embryonated eggs were infected with 10^3 PFU via the allantoic route. At 17 h (FPV) or 40 h (N) p.i., cryosections were prepared that were subjected to autoradiography after in situ hybridization with [^{35}S]UTP-labeled riboprobes directed against mRNA of H7 HA (a) and H10 HA (c). Sections of uninfected chick embryos were used as controls (b and d). Exposure time for autoradiography was 8 h.

control virus, usually died at 30 h p.i. without significant bleeding.

To determine spread of infection and organ tropism of these viruses, 20-μm sagittal sections of the embryos were subjected to in situ hybridization with specific radioactive riboprobes. Figure 1 shows autoradiograms of hybridized sections. All organs of the chicken embryo infected with FPV (Fig. 1a) were heavily labeled with the riboprobe, indicating that the virus caused systemic infection. In contrast, virus N caused only local infection of the allantoic membrane and of the cloaca connected with the allantoic cavity (Fig. 1c). Sections of uninfected embryos displayed only background staining (Figs. 1b and d).

Our next aim was to determine individual cell types within organs in which FPV replication takes place. To this end, sections of chicken embryos were analyzed at higher resolution. After in situ hybridization, slides were covered with photoemulsion, exposed for 2 days, developed, and counterstained with hematoxylin-eosin. The presence of viral RNA in all organs examined confirmed the pantropic character of the infection. It was interesting to see, however, that infection was confined in the organs almost exclusively to endothelial cells (Fig. 2). This is clearly indicated by the results obtained from a large blood vessel. Besides a few signals in peripheral blood cells, there was extensive endothelial labeling, whereas viral RNA was virtually absent in all other cells of the wall of the vessel (Fig. 2a). Distinct endothelial labeling patterns were also observed in lung, stomach, heart, and liver (Fig. 2b, c, d, and e). The hexagonal labeling pattern with the parabronchi in the center that was observed in the lung reflects the typical arrangement of developing blood vessels in this organ (Fig. 2b). In the stomach, HA-specific RNA was detected in endothelial cells of the vascularized submucosa as well as in endothelial cells of vessels within the stomach wall but not in epithelial cells (Fig. 2c). In the heart, the number of endothelial cells almost equals that of myocytes. Therefore, this organ was heavily infected with FPV, but again, only endothelial cells and not myocytes were stained by the HA-specific probe (Fig. 2d). In the liver, viral RNA was detectable in endothelium, whereas the columns of hepatocytes were not infected (Fig. 2e). The spleen, in contrast to other organs, showed a diffuse labeling pattern with the HA-specific riboprobe (Fig. 2f). This can be explained by the specific architecture of this organ, which does not possess a closed blood circulation, since the splenal sinusoids are lined by a discontinuous layer of endothelial cells.

To further assess the identity of endothelial cells and to confirm the concept that these cells are the specific target of FPV, we compared the labeling pattern of the HA-specific riboprobe with that of a riboprobe directed against the mRNA of vascular endothelial growth factor receptor 2 (VEGF receptor 2). VEGF receptor 2, which is expressed in rather small amounts and could therefore be visualized only by dark-field microscopy, is a protein involved in angiogenesis and is exclusively expressed in endothelial cells (9). The labeling patterns obtained by the VEGF receptor-specific riboprobe were essentially those obtained by the HA-specific probe. Thus, VEGF receptor 2 showed the typical hexagonal expression pattern in the lung, as did HA (cf. Fig. 3a and 2b), whereas, again like HA, it was diffusely expressed in spleen (cf. Fig. 3b and 2f). The in situ hybridization experiments therefore demonstrate clearly that endothelial cells are the main target of FPV in chicken embryos.

Linkage of endotheliotropism to FPV HA. To determine the genes responsible for endotheliotropism, we analyzed a set of reassortants of FPV and the apathogenic virus N (7) (Table 1). All reassortants except for 108 and 109 displayed the same endotheliotropism as wild-type FPV, although in some cases more than half of the RNA segments were derived from virus N (e.g., 118). In contrast to all other reassortants, reassortants 108 and 109 have the HA of virus N, which, unlike FPV HA, has restricted cleavability. Viral RNA from the two reassortants could not be detected in embryonic tissues, although they reached high HA titers ($\geqq 2^7$) within the allantoic fluid. This result is in good agreement with earlier studies showing a clear correlation between the cleavability of HA and spread of infection from the allantoic cavity into the embryo (27). In addition, it demonstrates that FPV HA is both necessary and sufficient for infection of endothelia.

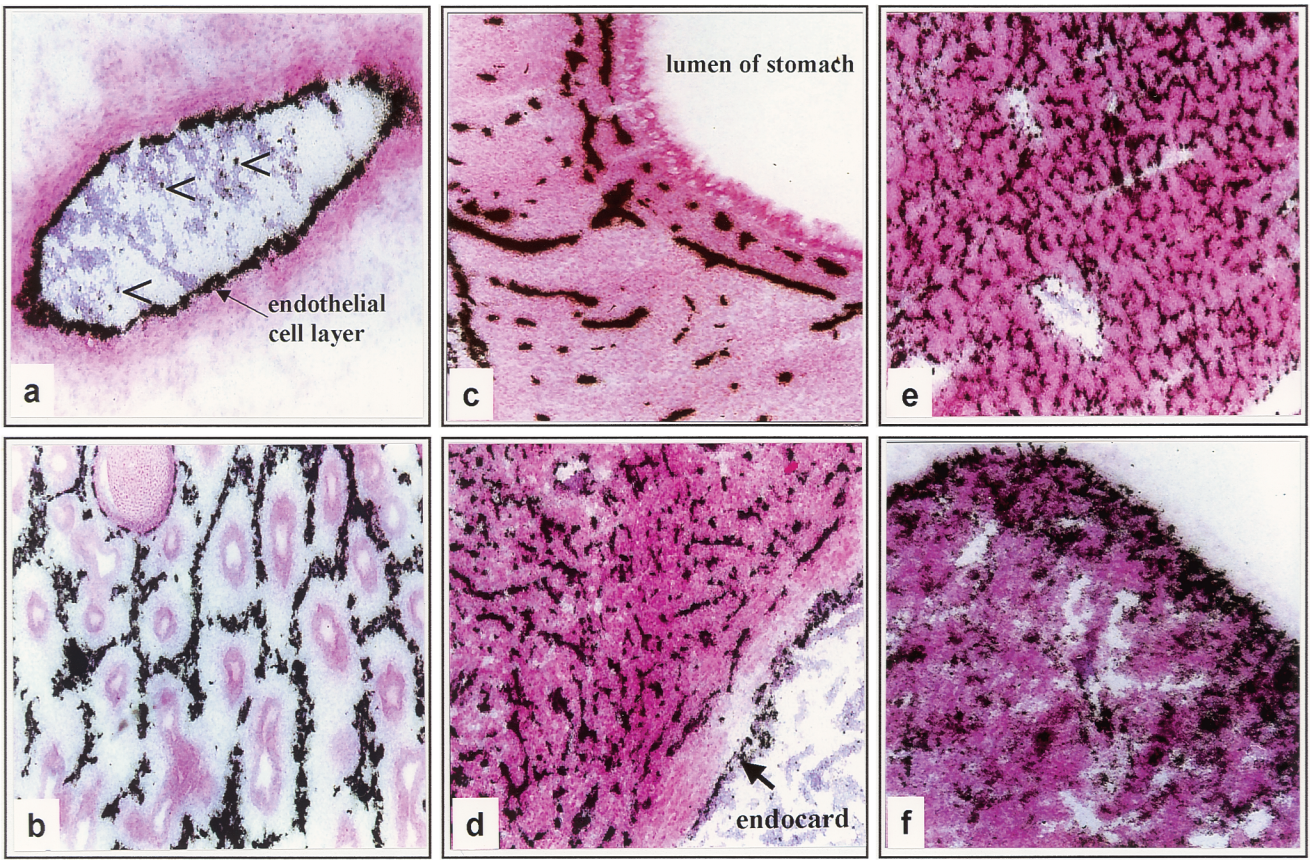

FIG. 2. Localization of FPV-infected cells in embryonic tissues by in situ hybridization. Bright-field photomicrographs showing autoradiograms with black grains representing bound HA-specific riboprobe in organs of the chick embryo. After in situ hybridization, slides were covered by photoemulsion, exposed for 2 days, developed, and counterstained by hematoxylin-eosin. (a) Blood vessel (arrowheads indicate infected blood cells); (b) lung; (c) stomach; (d) heart; (e) liver; (f) spleen. Magnification, ×57.

Identification and localization of proprotein convertases activating FPV HA in the chicken embryo. Proteolytic activation of the hemagglutinin by cellular proteases is an important factor determining spread of infection and organ tropism of influenza viruses. Although FPV HA is generally believed to be activated in most cells, it had to be excluded that confinement of FPV infection to endothelial cells is due to the absence of an appropriate protease in these cells. FPV HA is activated at its multibasic cleavage site by the proprotein convertases furin (33) and PC5/PC6 (14), as has been established in expression experiments in which cDNA clones of human or murine origin were used. To find out if these enzymes were also involved in replication and spread of FPV in its natural host, they first had to be identified in chicken tissue. By cloning cDNA from chicken liver RNA, we could show that chicken furin (gfur) displays all of the structural characteristics of human furin, including the propeptide that is autocatalytically removed by cleavage, the subtilisin-like domain with the active residues Asp, His, and Ser of the catalytic triad, the cysteine-rich domain, the transmembrane domain, and the cytoplasmic tail. By cloning gene fragments of gPC5/PC6, gLPC/PC7, and gPACE4, the presence of these proprotein convertases in chicken tissues has also been established.

To examine cleavage of HA by gfur, expression studies using recombinant vaccinia virus as the vector were carried out in the furin-deficient LoVo cell line (36). As shown in Fig. 4, gfur is expressed in these cells and able to cleave FPV HA.

It was then of interest to find out which proteases are expressed in endothelial cells of chicken embryos. To this end we analyzed the presence of proprotein convertase mRNA in feather germs of chicken embryos by in situ hybridization (Fig. 5). HA-specific viral RNA visualized by in situ hybridization served as a marker for endothelial cells in the center of the feather germs. It was absent in the surrounding epidermal layer. gfur- and gPC5/PC6-specific signals were seen in the epidermal region as well as in endothelial cells. No gLPC/PC7-specific hybridization signal could be detected in feather germs, while a large amount of gPACE4-specific mRNA was visible. Thus, furin and PC5/PC6, two potential activating proteases of FPV HA, are expressed in endothelial cells of the chicken embryo. High amounts of PACE4-specific mRNA were also observed within the cells of the feather germs, but this protease probably plays a minor role as an activating protease of FPV HA (14).

To analyze cleavage in isolated endothelial cells, we infected HUVEC cells with FPV, since chicken endothelia are difficult to culture. The presence of the proprotein convertase PC5/PC6 in HUVEC has been shown before (3). By Northern blot analysis and RT-PCR, we could also show the expression of furin and LPC/PC7 in HUVEC (data not shown). FPV replicates well in HUVEC (Fig. 6A). The analysis of released virus particles indicated that HA is readily cleaved in these cells (Fig. 6B). Taken together, the results shown in Fig. 4, 5, and 6 indicate that the limitation of the infection to endothelial cells

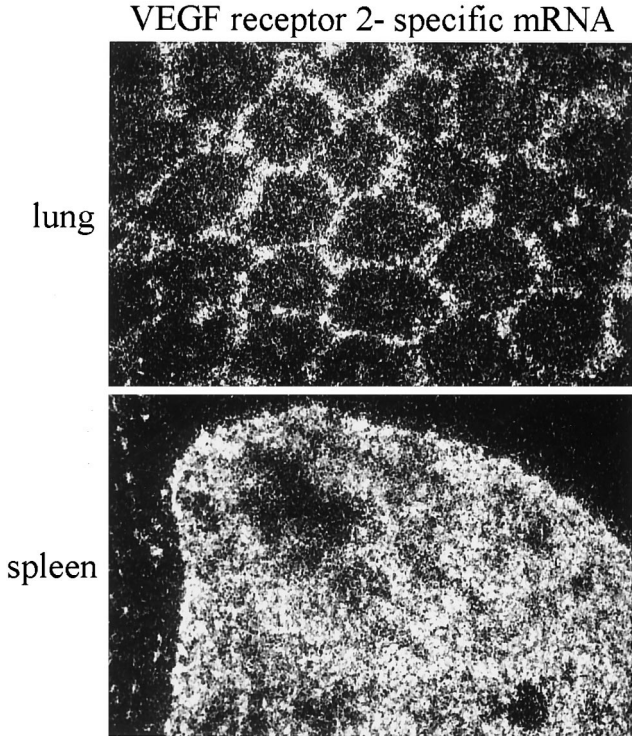

FIG. 3. Identification of endothelia by in situ hybridization using VEGF receptor 2 as a marker. Dark-field microscopy showing autoradiographic silver grains representing bound VEGF receptor 2-specific mRNA in lung and spleen of chick embryos. After in situ hybridization with a radioactive probe directed against mRNA of VEGF receptor 2, the slides were covered by photoemulsion, exposed for 30 days, and developed. Magnification, ×71.

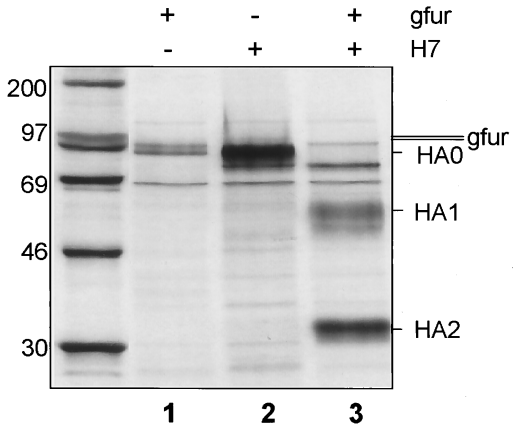

FIG. 4. Cleavage of HA by chicken furin. LoVo cells (35) were infected with VV:gfur and VV:HAwt (22), each at an MOI of 10. Virus inocula were replaced by DMEM without FCS 1 h after infection. At 4 h after infection, LoVo cells (diameter of the culture dishes, 35 mm) were starved for methionine for 1 h and then labeled with 100 μCi of [^{35}S]methionine (1,000 Ci/mmol; Amersham, Braunschweig, Germany) for 3 h in 0.5 ml of methionine-free MEM. The medium was replaced by MEM containing nonradioactive methionine, and incubation was continued for an additional hour. Cells were lysed in radioimmunoprecipitation buffer. After immunoprecipitation with anti-FPV or anti-hfur rabbit serum (final dilution, 1:500) and protein A-Sepharose CL-4B (Sigma, Deisenhofen, Germany), proteins were analyzed by SDS–10% PAGE under reducing conditions. Sizes are shown in kilodaltons.

cannot be explained by the absence of activating proteases within these cells or in adjacent tissues.

Expression of viral receptors in embryonic tissues. Since little was known about the role of the host cell receptor in tissue tropism, we investigated cell-specific expression of neuraminic acid in the chick embryo. This was done by histochemical analysis employing MAA, specific for NeuAc-α2,3-Gal, the preferential receptor of avian influenza viruses, and SNA, specific for NeuAc-α2,6-Gal, the receptor determinant favored by mammalian strains. It has to be pointed out that these lectins react only with protein-bound oligosaccharides. There is therefore no information from our experiments on a possible role of gangliosides as receptors. Figure 7 shows the results obtained with lung and liver. Labeling of lung tissue with SNA yielded the characteristic hexagonal endothelial pattern that was also observed after in situ hybridization with the HA-specific probe. In contrast, MAA bound exclusively to the epithelia of the parabronchi that were not infected (cf. Fig. 2b). Several conclusions can be drawn from these observations. First, they show that NeuAc-α2,6-Gal can serve as a receptor for FPV and that it specifically mediates infection of lung endothelia. Second, endothelial and epithelial cells of the lung of an 11-day-old chicken embryo contain FPV receptors, although only the former are infected. The data shown in Fig. 7 demonstrate furthermore that, at least with the methods employed in this work, neuraminic acid cannot be detected in mesenchymal cells between the endothelial and epithelial cells of the alveolae. Thus, it appears that mesenchymal cells have a barrier function preventing spread of infection from the endothelia to the alveolae.

When liver tissue was analyzed with the SNA probe, the continuous layer of endothelial cells lining the sinusoids was stained, indicating that these cells contain NeuAc-α2,6-Gal, as is the case in the lung. A different staining pattern was again obtained when MAA was used. The cells labeled with this lectin extended into the lumen of the sinusoids, most likely representing Kupffer cells. It therefore appears that Kupffer cells specifically express NeuAc-α2,3-Gal. These data indicate that in liver tissue, virus receptors are expressed only on cells facing the lumen of the sinusoids, whereas they could not be detected on hepatocytes. Thus, the distribution of virus receptors in the liver corresponds exactly to the pattern of virus infection (cf. Fig. 2e), again suggesting that expression of neuraminic acid receptors is an important determinant for the endotheliotropism of FPV.

Polarized maturation of FPV in endothelial cells. As has been pointed out already in the Introduction, an important factor for virus spread is the polarized release of virions from infected cells. When we analyzed the heart of an infected chick embryo by electron microscopy, we could confirm polar bud-

TABLE 1. Gene constellation and endotheliotropism of reassortants of FPV and virus N

Virus	Origin of gene								Endotheliotropism
	PB1	PB2	PA	HA	NP	NA	MS1 and MS2	NS1 and NS2	
106	**N**	FPV	FPV	FPV	FPV	FPV	FPV	FPV	+
111	FPV	**N**	FPV	FPV	FPV	FPV	FPV	FPV	+
116	FPV	FPV	**N**	FPV	FPV	FPV	FPV	FPV	+
114	FPV	FPV	FPV	FPV	**N**	FPV	FPV	FPV	+
110	FPV	FPV	FPV	FPV	FPV	**N**	FPV	FPV	+
118	FPV	**N**	**N**	FPV	**N**	**N**	FPV	FPV	+
119	FPV	**N**	**N**	FPV	**N**	FPV	FPV	**N**	+
122	FPV	FPV	**N**	FPV	FPV	**N**	**N**	**N**	+
108	FPV	**N**	**N**	**N**	**N**	FPV	FPV	FPV	−
109	FPV	FPV	**N**	**N**	**N**	FPV	FPV	FPV	−

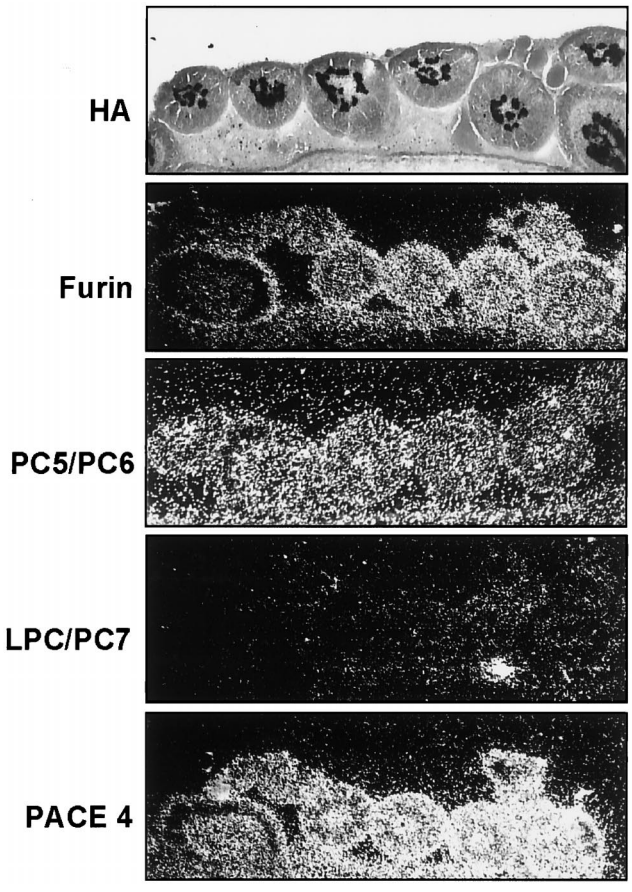

FIG. 5. Localization and identification of FPV and proprotein convertases in feather germs by in situ hybridization. For the analysis of proprotein convertases, cryosections of uninfected chicken embryos were incubated with [^{35}S]UTP-labeled riboprobes directed against mRNA of the proteases. Slides were covered by photoemulsion, exposed for 21 days, developed, and inspected by dark-field microscopy. For analysis of FPV-infected cells, cryosections prepared at 17 h p.i. were subjected to in situ hybridization with an HA-specific probe, covered with photoemulsion, exposed for 2 days, developed, stained with hematoxylin-eosin, and inspected by bright-field microscopy. Magnification, ×75.

ding of FPV from endothelial cells. Virus particles were present exclusively at the apical part of the cell membrane; no budding virus was detected at the basolateral side (Fig. 8).

We then examined the expression of HA at the surface of infected HUVEC grown on Transwell filters. Figure 9A shows the results obtained by confocal laser scanning microscopy. HA-specific fluorescence was distributed all over the cell surface when inspected from the top. Examination of sagittal sections revealed selective staining of the apical membrane. HA-specific fluorescence was not observed at the basal membrane below the nucleus. Finally, we analyzed HA by an assay for the selective biotinylation of surface proteins (19). In Fig. 9B we show that biotinylated FPV HA was immunoprecipitated almost exclusively from apically labeled cell lysates indicating a strong targeting of HA to the apical cell membrane. In contrast, VSV G protein, known to be transported to the basolateral side of polarized epithelial cells (23), was detected predominantly on the basal side of endothelial cells.

Taken together, the data shown in Fig. 8 and 9 indicate that HA is targeted exclusively to the luminal surface of endothelial cells and that virus budding also occurs only at this side. Thus, the polarity of virus maturation in endothelial cells may be another factor promoting spread of infection via the blood while hindering infection of subendothelial tissues.

DISCUSSION

We have found in this study that FPV shows strict endotheliotropism when infecting 11-day-old chick embryos. Since hemorrhages and edema are major symptoms in FPV-infected chickens, it was not unexpected to see that the vasculature is an important target of infection. However, we were surprised when we could not detect viral replication in other cell types. Besides endothelia, myocytes and lymphatic tissues were found to be sites of virus replication when hatched chickens were infected with other pathogenic H5 and H7 strains (17, 39, 40). These differences in cell tropism may depend on the developmental stage of the host and on the virus strains used.

The results obtained with the reassortants of FPV and virus N clearly indicate that endotheliotropism requires the pres-

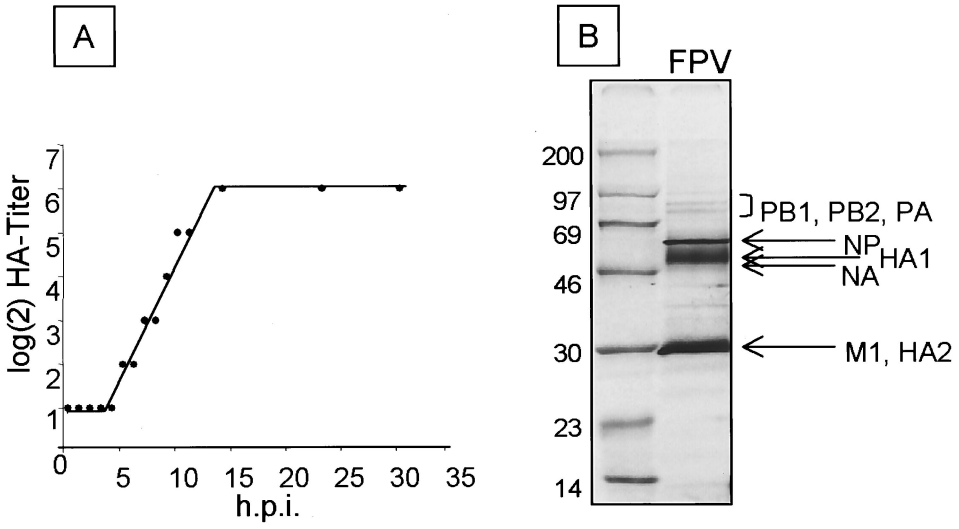

FIG. 6. Replication of FPV in HUVEC. (A) Confluent cell layer of HUVEC was infected with egg-grown FPV at an MOI of 1. Release of virus was measured by hemagglutinating activity in the supernatant. (B) Autoradiography of [^{35}S]methionine-labeled proteins of virus particles purified from the supernatant of infected HUVEC. At 20 h p.i., virus in the cell supernatant was centrifuged through a 20% sucrose cushion, and purified virus was disrupted in sample buffer containing 2% 2-mercaptoethanol and separated on a 10% polyacrylamide gel followed by autoradiography. Sizes are shown in kilodaltons.

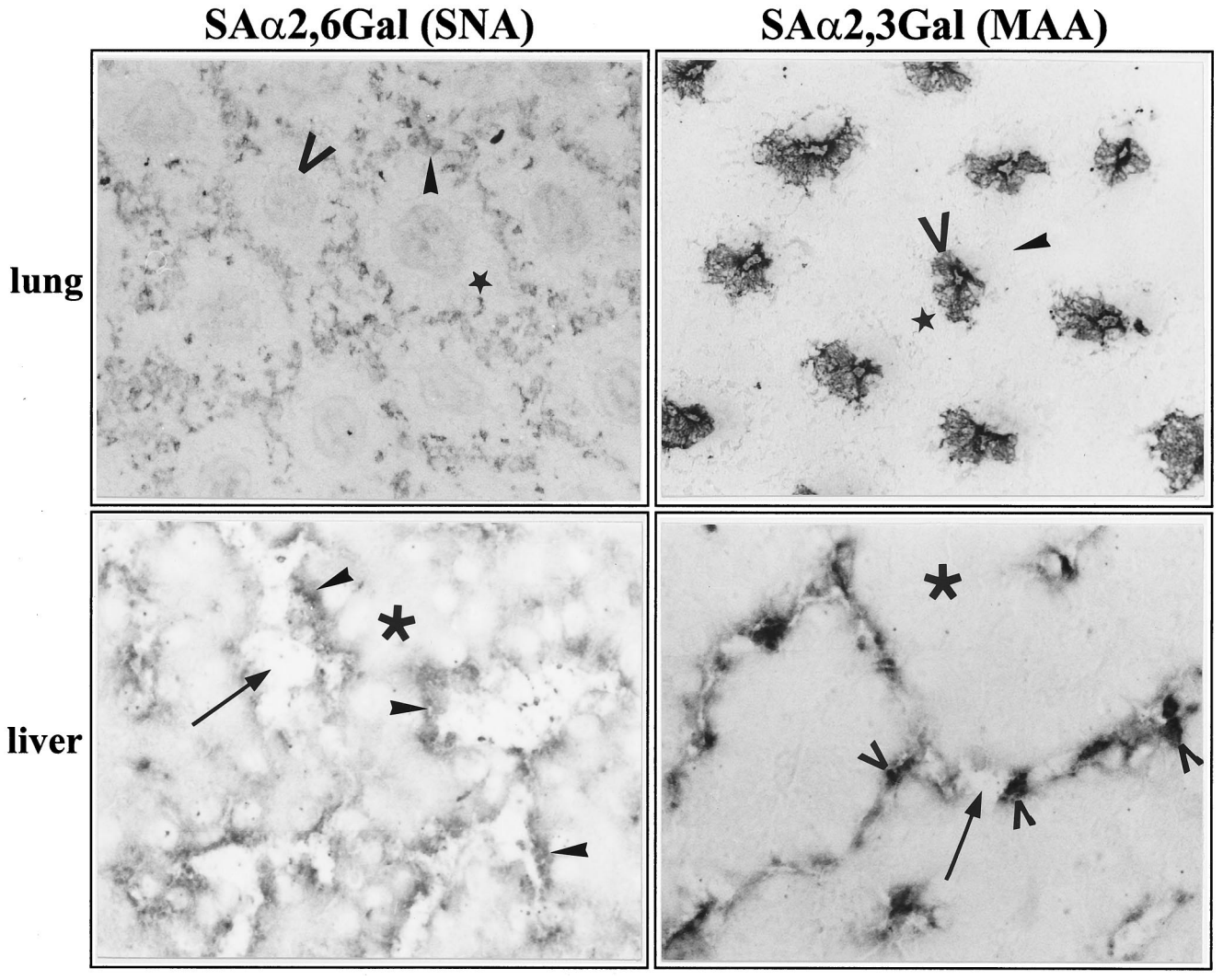

FIG. 7. Histochemical analysis of NeuAc-α2,3-Gal and NeuA-cα2,6-Gal in the lung and the liver of chicken embryos by lectin binding. Cryosections of uninfected chicken embryos were incubated with MAA, specific for NeuAc-α2,3-Gal, or SNA, specific for NeuAc-α2,6-Gal, as described in Materials and Methods. Bound lectins were identified using the DIG-glycan differentiation kit (Boehringer). Magnifications: ×75x and ×150 (liver). Symbols in lung sections indicate endothelial cells (solid arrowheads), mesenchymal cells (stars), alveolar and epithelia (open arrowheads). Symbols in liver sections indicate endothelial cells (solid arrowheads), Kupffer cells (open arrowheads), hepatocytes (asterisks), and sinusoids (arrows).

ence of FPV HA. This observation is in line with the concept that, because of its susceptibility to ubiquitous proteolytic activation, FPV HA allows virus entry from the allantoic cavity into the highly vascularized mesenchymal layer of the chorioallantoic membrane and thus mediates hematogenic spread of infection. On the other hand, the restricted cleavability of virus N HA confines infection to the inner layer of the membrane and the allantoic cavity (27). Reassortants containing virus N HA therefore did not have access to endothelia when infecting through the chorioallantoic route.

Whereas cleavage activation of HA proved to be essential for targeting the virus to endothelia, it was not responsible for confining the infection to these cells. To demonstrate this, we first had to clone gfur, gPC5/PC6, gLPC/PC7, and gPACE4, since none of the proprotein convertases had been identified before in the natural host of FPV. All of these proteases, which showed 70 to 96% nucleotide sequence homology to their mammalian analogues, were expressed in the chicken embryo. Furin and PC5/PC6, known to activate FPV HA when originating from mammalian species (14, 33), were identified in all chicken tissues analyzed, including endothelial cells. These enzymes had also been detected in murine and human endothelia (2, 3). Furthermore, we showed that gfur is able to cleave FPV HA and that cultured endothelia allow productive FPV infection. Taken together, these observations indicate that the lack of spread of infection from endothelia to surrounding tissues cannot be attributed to the absence of activating proteases.

In contrast, tissue-specific expression of virus receptors appears to be an important factor in restricting infection to endothelia. With the lectin-binding assays employed in this study, we could detect α2,3-linked and α2,6-linked neuraminic acid, both of which proved to be able to serve as FPV receptors only on epithelial cells and on cells of the reticuloendothelial system.

Similar results have been obtained in a study on the brain microvasculature of the chicken embryo, in which another neuraminic acid-binding lectin was shown to selectively bind to the luminal side of the endothelia (21). However, with the

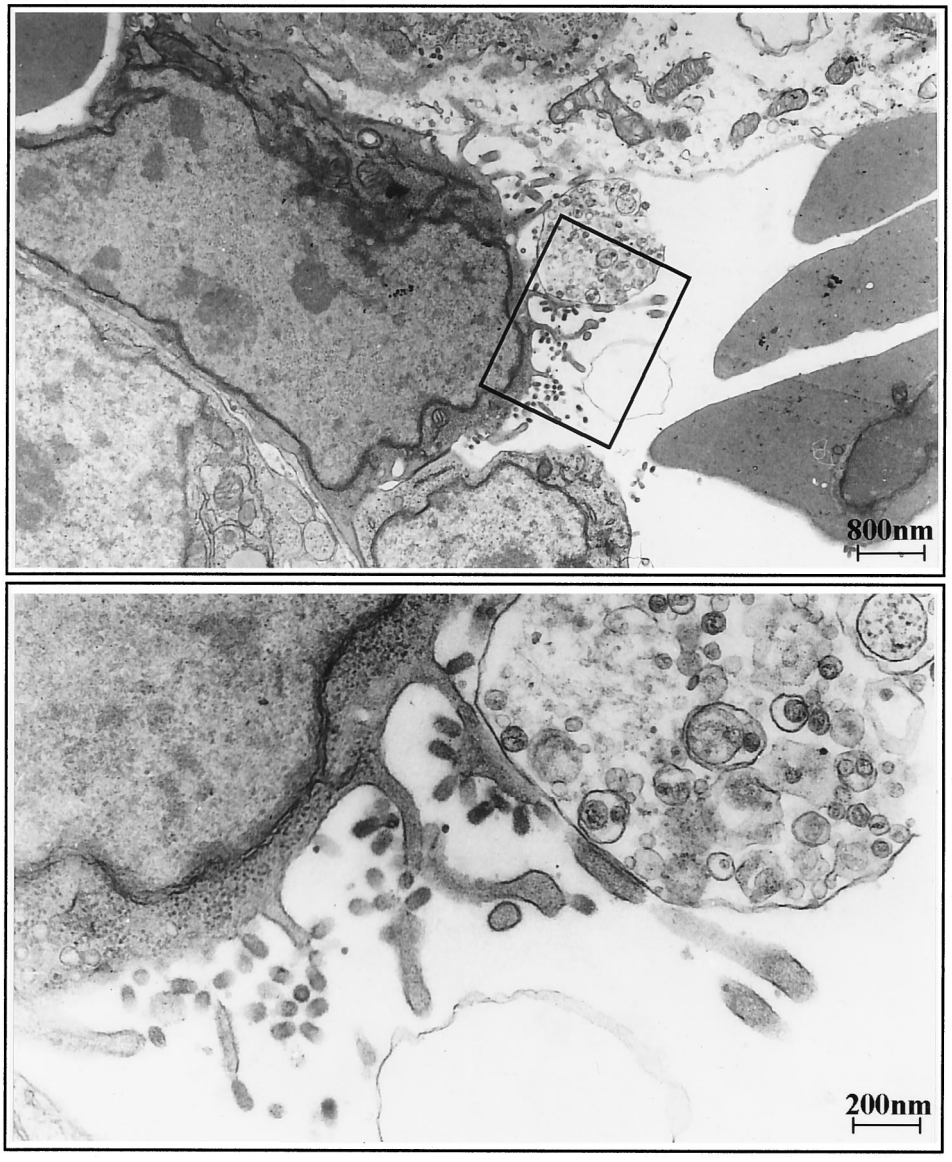

FIG. 8. Electron micrograph of an FPV-infected endothelial cell from a heart capillary. At 18 h p.i., the heart of an infected chicken embryo was prepared for transmission electron microscopy. (Top) Numerous virus particles bud from the luminal side of the endothelial cell. (Bottom) The section boxed in the top panel at higher magnification.

methods employed here, we could not detect receptor determinants on other cells, such as myocytes, fibroblasts, and hepatocytes. Thus, it appears that cells lacking a measurable number of neuraminic acid receptors cannot be infected by FPV and are therefore a barrier to the spread of infection. This concept is nicely supported by the observations made on lung tissue. When this organ is infected via the hematogenic route, as is the case in the embryo at day 11, the virus is retained in the endothelial cells of the capillary vessels. Since neuraminic acid is present in α2,6 linkage on these cells, it is clear that this type of neuraminic acid can serve as an FPV receptor, although it appears that binding of avian strains is generally determined by the α2,3 linkage. The alveolar epithelia, although expressing the virus receptor in large amounts, are not infected because virus access is prevented by the connective tissue lacking neuraminic acid. On the other hand, when embryos are infected through the airways, as can be done by inoculating virus 2 days before hatching into the now almost dry allantoic cavity, virus replication is readily detected in lung epithelia (data not shown).

It has to be pointed out that expression of neuraminic acid in the chick embryo depends on tissue differentiation (4). This may explain the absence of detectable amounts of neuraminic acid on fibroblasts in situ, whereas cultured fibroblasts readily express receptors, as indicated by their ability to allow efficient virus replication. It also has to be assumed that the subendothelial connective tissue is not a very tight barrier in the choriallantoic membrane, where it allows penetration of the virus from the allantoic epithelium into the mesodermal endothelia. In fact, small amounts of virus budding from mesodermal fibroblasts have been observed, indicating that these cells may play a role in mediating spread of infection (27). Whether the spread through the mesodermal layer is driven by the particularly high virus replication rates in the allantoic epithelium

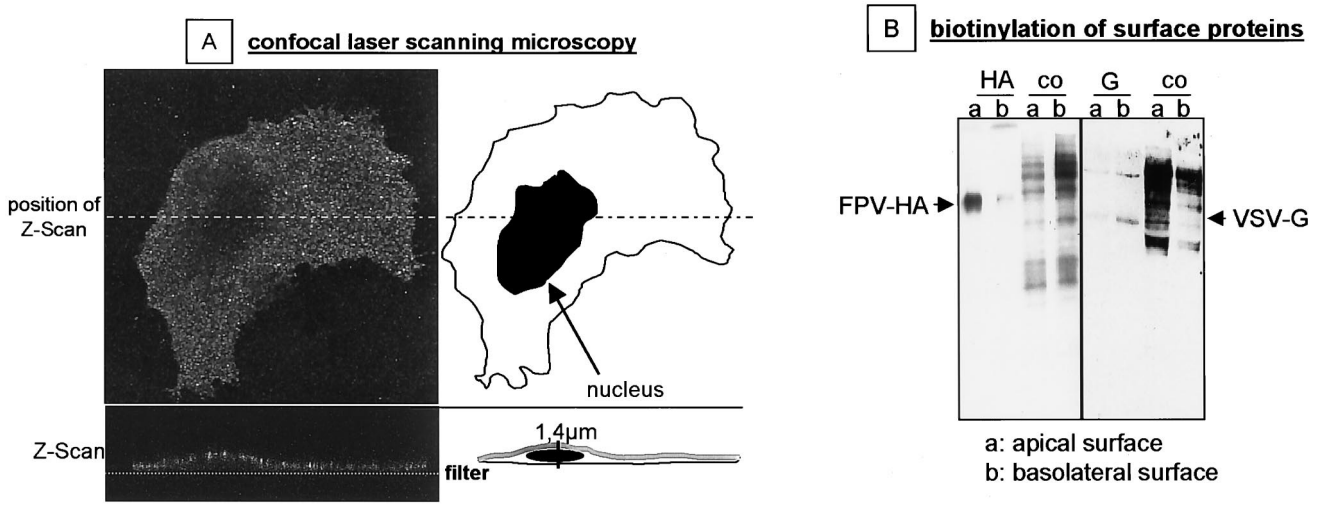

FIG. 9. Polarized expression of HA at the luminal side of FPV-infected HUVEC. (A) HUVEC were grown on Transwell filters. At 4 h p.i. with FPV, they were analyzed by confocal laser scanning microscopy using an HA-specific monoclonal antibody (HA1-A11H7) for immunofluorescence labeling. Magnification, ×630. (B) Distribution of viral glycoproteins on the apical (a) and basolateral (b) surfaces of HUVEC infected with either FPV or VSV. Surface proteins were labeled by domain-specific biotinylation and immunoprecipitated using the monoclonal antibody against FPV HA or a polyclonal antiserum against VSV (for details, see Materials and Methods).

and the presence of neuraminic acid on mesodermal fibroblasts or by some other mechanism remains to be seen.

Our data also show that the polarity of virus budding is another factor contributing to the confinement of infection to endothelial cells. Studies on Sendai virus in a mouse model have shown before that the sidedness of virus maturation has a distinct effect on spread of infection in the organism and on pathogenicity. Wild-type Sendai virus released exclusively from the apical surface of lung epithelia is strictly pneumotropic, whereas the mutant F1-R, which matures at the apical as well as the basolateral side, causes pantropic infection (37, 38). It has long been known that FPV matures preferentially at the luminal side of endothelia (27), and the observations made here on virus budding and HA transport support this concept. The luminal budding polarity of FPV therefore supports the hematogenic spread of the virus and at the same time prevents infection of subendothelial cells.

Finally, we have obtained evidence that the architecture of the endothelia also plays a role in virus spread. Whereas endothelia form a continuous cell layer in most organs, they are fenestrated in the liver and spleen. Our data show that the endothelial gaps have little effect on FPV dissemination in the liver because the underlying hepatocytes are resistant to infection. The spleen, however, does not have such a barrier beneath the endothelia. The virus can therefore spread freely within this organ, as indicated by the diffuse in situ hybridization pattern.

Taken together, our data indicate that endotheliotropism of FPV in the chick embryo is the result of an interplay of several factors determined by the virus and the host. These include proteolytic activation of HA by ubiquitous proteases, which is responsible for entry of the virus into the vascular system, and at least two mechanisms contributing to the confinement of the virus to endothelia: the polarity of virus budding at the luminal side of endothelial cells and cell-specific differences in the expression of neuraminic acid receptors. Endotheliotropism without doubt plays an important role in the generalization of FPV infection and in the generation of typical symptoms of the disease, such as hemorrhages and edema. Systemic infection and severe vascular injury are also the central pathogenetic mechanisms of hemorrhagic fevers in primates caused by filoviruses and other agents, and there is evidence that at least some of these viruses also replicate in endothelia (28, 30, 43). It will therefore be interesting to see if mechanisms similar to those described here for FPV infection also play a role in the pathogenesis of hemorrhagic fevers in other species.

ACKNOWLEDGMENTS

We are grateful to R. Rott and C. Scholtissek, Giessen, for helpful discussions and for providing influenza virus reassortants. We thank E. Weihe for support in autoradiographic and microscopic techniques. The electron micrographs were made by B. Agricola.

This study was supported by grants from the Deutsche Forschungsgemeinschaft (SFB 286 and KL 238/6-1) and from the Fonds der Chemischen Industrie.

REFERENCES

1. **Banks, J., E. Speidel, and D. J. Alexander.** 1998. Characterization of an avian influenza A virus isolated from a human—is an intermediate host necessary for the emergence of pandemic influenza viruses? Arch. Virol. **143:**781–787.
2. **Beaubien, G., M. K. Schafer, E. Weihe, W. Dong, M. Chretien, N. G. Seidah, and R. Day.** 1995. The distinct gene expression of the pro-hormone convertases in the rat heart suggests potential substrates. Cell Tissue Res. **279:**539–549.
3. **Campan, M., M. Yoshizumi, N. G. Seidah, M. E. Lee, C. Bianchi, and E. Haber.** 1996. Increased proteolytic processing of protein tyrosine phosphatase mu in confluent vascular endothelial cells: the role of PC5, a member of the subtilisin family. Biochemistry **35:**3797–3802.
4. **Codogno, P., and M. Aubery.** 1983. Changes in cell-surface sialic acid content during chick embryo development. Mech. Ageing Dev. **23:**307–314.
5. **Connor, R. J., Y. Kawaoka, R. G. Webster, and J. C. Paulson.** 1994. Receptor specificity in human, avian, and equine H2 and H3 influenza virus isolates. Virology **205:**17–23.
6. **de Jong, J. C., E. C. Claas, A. D. Osterhaus, R. G. Webster, and W. L. Lim.** 1997. A pandemic warning? Nature **389:**554.
7. **Dinter, Z., and J. Bakos.** 1950. Ueber die Beziehungen des Virus N zu dem Virus der klassischen Gefluegelpest. Berl. Muench. Tieraerztl. Wochenschr. **63:**101–105.
8. **Feldmann, H., E. Kretzschmar, B. Klingeborn, R. Rott, H. D. Klenk, and W. Garten.** 1988. The structure of serotype H10 hemagglutinin of influenza A virus: comparison of an apathogenic avian and a mammalian strain pathogenic for mink. Virology **165:**428–437.
9. **Flamme, I., G. Breier, and W. Risau.** 1995. Vascular endothelial growth factor (VEGF) and VEGF receptor 2 (flk-1) are expressed during vasculogenesis and vascular differentiation in the quail embryo. Dev. Biol. **169:**699–712.

10. **Gambaryan, A. S., A. B. Tuzikov, V. E. Piskarev, S. S. Yamnikova, D. K. Lvov, J. S. Robertson, N. V. Bovin, and M. N. Matrosovich.** 1997. Specification of receptor-binding phenotypes of influenza virus isolates from different host using synthetic sialylglycopolymers: non-egg-adapted human H1 and H3 influenza A and influenza B viruses share a common high binding affinity for 6′-sialyl(N-acetyllactosamine). Virology **232:**345–350.
11. **Garten, W., D. Linder, R. Rott, and H. D. Klenk.** 1982. The cleavage site of the hemagglutinin of fowl plague virus. Virology **122:**186–190.
12. **Gimbrone, M. A. J., R. S. Cotran, and J. Folkman.** 1974. Human vascular endothelial cells in culture. Growth and DNA synthesis. J. Cell Biol. **60:**673–684.
13. **Gratzl, E., and H. Koehler.** 1968. Gefluegelpest, p. 178–200. *In* Spezielle Pathologie und Therapie der Gefluegelkrankheiten. Ferdinand Enke Verlag, Stuttgart, Germany.
14. **Horimoto, T., K. Nakayama, S. P. Smeekens, and Y. Kawaoka.** 1994. Proprotein-processing endoproteases PC6 and furin both activate hemagglutinin of virulent avian influenza viruses. J. Virol. **68:**6074–6078.
15. **Karnovsky, M. J.** 1968. The ultrastructural basis of transcapillary exchanges. J. Gen. Physiol. **52**(Suppl.)**:**95.
16. **Klenk, H. D., and W. Garten.** 1994. Activation cleavage of viral spike proteins by host proteases, p. 241–280. *In* E. Wimmer (ed.), Cellular receptors for animal viruses. Cold Spring Harbor Laboratory Press, Cold Spring Harbor, N.Y.
17. **Kobayashi, Y., T. Horimoto, Y. Kawaoka, D. Alexander, and C. Itakura.** 1996. Pathological studies of chickens experimentally infected with two highly pathogenic avian influenza viruses. Avian Pathol. **25:**285–304.
18. **Kurtz, I., R. J. Manvell, and J. Banks.** 1996. Avian influenza virus isolated from a woman with conjunctivitis. Lancet **348:**901–902.
19. **Lisanti, M. P., M. Sargiacomo, L. Graeve, A. R. Saltiel, and E. Rodriguez-Boulan.** 1988. Polarized apical distribution of glycosyl-phosphatidylinositol-anchored proteins in a renal epithelial cell line. Proc. Natl. Acad. Sci. USA **85:**9557–9561.
20. **Narayan, O., J. Thorsen, T. J. Hulland, G. Ankeli, and P. G. Joseph.** 1972. Pathogenesis of lethal influenza virus infection in turkeys. I. Extraneural phase of infection. J. Comp. Pathol. **82:**129–137.
21. **Nico, B., F. Quondamatteo, D. Ribatti, M. Bertossi, G. Russo, R. Herken, and L. Roncali.** 1998. Ultrastructural localization of lectin binding sites in the developing brain microvasculature. Anat. Embryol. (Berlin) **197:**305–315.
22. **Roberts, P. C., W. Garten, and H. D. Klenk.** 1993. Role of conserved glycosylation sites in maturation and transport of influenza A virus hemagglutinin. J. Virol. **67:**3048–3060.
23. **Rodriguez-Boulan, E., K. T. Paskiet, and D. D. Sabatini.** 1983. Assembly of enveloped viruses in Madin-Darby canine kidney cells: polarized budding from single attached cells and from clusters of cells in suspension. J. Cell Biol. **96:**866–874.
24. **Rogers, G. N., and B. L. D'Souza.** 1989. Receptor binding properties of human and animal H1 influenza virus isolates. Virology **173:**317–322.
25. **Rogers, G. N., and J. C. Paulson.** 1983. Receptor determinants of human and animal influenza virus isolates: differences in receptor specificity of the H3 hemagglutinin based on species of origin. Virology **127:**361–373.
26. **Rott, R., M. Orlich, and C. Scholtissek.** 1979. Correlation of pathogenicity and gene constellation of influenza A viruses. III. Non-pathogenic recombinants derived from highly pathogenic parent strains. J. Gen. Virol. **44:**471–477.
27. **Rott, R., M. Reinacher, M. Orlich, and H. D. Klenk.** 1980. Cleavability of hemagglutinin determines spread of avian influenza viruses in the chorioallantoic membrane of chicken embryo. Arch. Virol. **65:**123–133.
28. **Ryabchikova, E. J., L. V. Kolesnikova, and S. V. Netesov.** 1999. Animal pathology of filoviral infections. Curr. Top. Microbiol. Immunol. **235:**145–173.
29. **Schaefer, M. K., and R. Day.** 1995. In situ hybridization techniques to map processing enzymes. Methods Neurosci. **23:**16–44.
30. **Schnittler, H. J., F. Mahner, D. Drenckhahn, H.-D. Klenk, and H. Feldmann.** 1993. Replication of Marburg virus in human endothelial cells. A possible mechanism for the development of viral hemorrhagic disease. J. Clin. Investig. **91:**1301–1309.
31. **Scholtissek, C., I. Koennecke, and R. Rott.** 1978. Host range recombinants of fowl plague (influenza A) virus. Virology **91:**79–85.
32. **Scholtissek, C., and B. R. Murphy.** 1978. Host range mutants of an influenza A virus. Arch. Virol. **58:**323–333.
33. **Stieneke-Gröber, A., M. Vey, H. Angliker, E. Shaw, G. Thomas, C. Roberts, H. D. Klenk, and W. Garten.** 1992. Influenza virus hemagglutinin with multibasic cleavage site is activated by furin, a subtilisin-like endoprotease. EMBO J. **11:**2407–2414.
34. **Suarez, D. L., M. L. Perdue, N. Cox, T. Rowe, C. Bender, J. Huang, and D. E. Swayne.** 1998. Comparisons of highly virulent H5N1 influenza A viruses isolated from humans and chickens from Hong Kong. J. Virol. **72:**6678–6688.
35. **Subbarao, K., A. Klimov, J. Katz, H. Regnery, W. Lim, H. Hall, M. Perdue, D. Swayne, C. Bender, J. Huang, M. Hemphill, T. Rowe, M. Shaw, X. Xu, K. Fukuda, and N. Cox.** 1998. Characterization of an avian influenza A (H5N1) virus isolated from a child with fatal respiratory illness. Science **279:**393–396.
36. **Takahashi, S., T. Nakagawa, K. Kasai, T. Banno, S. J. Duguay, W. J. Van de Ven, K. Murakami, and K. Nakayama.** 1995. A second mutant allele of furin in the processing-incompetent cell line LoVo: evidence for involvement of the homo B domain in autocatalytic activation. J. Biol. Chem. **270:**26565–26569.
37. **Tashiro, M., J. T. Seto, S. Choosakul, M. Yamakawa, H. D. Klenk, and R. Rott.** 1992. Budding site of Sendai virus in polarized epithelial cells is one of the determinants for tropism and pathogenicity in mice. Virology **187:**413–422.
38. **Tashiro, M., M. Yamakawa, K. Tobita, J. T. Seto, H. D. Klenk, and R. Rott.** 1990. Altered budding site of a pantropic mutant of Sendai virus, F1-R, in polarized epithelial cells. J. Virol. **64:**4672–4677.
39. **van Campen, H., B. C. Easterday, and V. S. Hinshaw.** 1989. Destruction of lymphocytes by a virulent avian influenza A virus. J. Gen. Virol. **70:**467–472.
40. **van Campen, H., B. C. Easterday, and V. S. Hinshaw.** 1989. Virulent avian influenza A viruses: their effect on avian lymphocytes and macrophages in vivo and in vitro. J. Gen. Virol. **70:**2887–2895.
41. **Vey, M., W. Schäfer, S. Berghofer, H. D. Klenk, and W. Garten.** 1994. Maturation of the trans-Golgi network protease furin: compartmentalization of propeptide removal, substrate cleavage, and COOH-terminal truncation. J. Cell Biol. **127:**1829–1842.
42. **Webster, R. G., W. J. Bean, O. T. Gorman, T. M. Chambers, and Y. Kawaoka.** 1992. Evolution and ecology of influenza A viruses. Microbiol. Rev. **56:**152–179.
43. **Zaki, S. R., and C. S. Goldsmith.** 1999. Pathologic features of filovirus infections in humans. Curr. Top. Microbiol. Immunol. **235:**97–116.